Current Biology 16, 1502–1508, August 8, 2006 ©2006 Elsevier Ltd All rights reserved DOI 10.1016/j.cub.2006.05.064

Report

Control of Cardiac Rhythm by ORK1, a *Drosophila* Two-Pore Domain Potassium Channel

Nathalie Lalevée,[1,2] Bruno Monier,[1,2] Sébastien Sénatore,[1] Laurent Perrin,[1] and Michel Sémériva[1,*]
[1] Institut de Biologie du Développement de Marseille-Luminy
UMR 6216 CNRS-Université de la Méditerranée
Case 907
Parc Scientifique de Luminy
13288 Marseille Cedex 9
France

Summary

Unravelling the mechanisms controlling cardiac automatism is critical to our comprehension of heart development and cardiac physiopathology. Despite the extensive characterization of the ionic currents at work in cardiac pacemakers, the precise mechanisms initiating spontaneous rhythmic activity and, particularly, those responsible for the specific control of the pacemaker frequency are still matters of debate and have not been entirely elucidated [1–4]. By using *Drosophila* as a model animal to analyze automatic cardiac activity, we have investigated the function of a K^+ channel, ORK1 (outwardly rectifying K^+ channel-1) in cardiac automatic activity. ORK1 is a two-pore domain K^+ (K2P) channel, which belongs to a diverse and highly regulated superfamily of potassium-selective leak channels thought to provide baseline regulation of membrane excitability. Cardiac-specific inactivation of *Ork1* led to an increase in heart rhythm. By contrast, when overexpressed, ORK1 completely prevented heart beating. In addition, by recording action potentials, we showed that the level of *Ork1* activity sets the cardiac rhythm by controlling the duration of the slow diastolic depolarization phase. Our observations identify a new mechanism for cardiac rhythm control and provide the first demonstration that K2P channels regulate the automatic cardiac activity.

Results and Discussion

In *Drosophila*, the cardiovascular system consists of an open circulatory system composed by 52 pairs of myocytes that are both endothelial and muscle cells organized in a tubular structure. The organ is divided into two distinct morphological and functional domains along the anterior-posterior axis: the aorta, which constitutes the outflow tract, and the heart itself, which is the only domain capable of spontaneous rhythmic activity (Figures 1A–1C, see Movie S1 in the Supplemental Data available with this article online). The heart, whose automatic myogenic activity regulates cardiac rhythm, ensures the circulation of hemolymph (Figure 1; Movie S1).

Axial information provided by the Hox genes, in combination with segmental information, assigns a unique positional identity to each myocyte and guides cells toward their specific differentiation pathway [5–7].

Ork1 Is Expressed in the Spontaneous Contracting Myocytes of the Larval Heart

To identify genes involved in automatic cardiac activity, we screened for genes that are specifically expressed in the contractile myocytes of the heart but not in the aorta myocytes. Among them, we characterized the genes encoding the Na^+-dependent bicarbonate anion exchanger 1 (NDAE1) [6], the unique *Drosophila* hyperpolarization channel nucleotide gated (HCN) [8] generating the cardiac pacemaker f current [9], and ORK1 (this study, Figure 1D).

ORK1 (KCNKO) is one of the first members of the two-pore domain potassium (K2P) channel superfamily identified in a pluricellular organism and has been biophysically characterized [10–12]. ORK1 displays the attributes expected for leak channels and shows macroscopic currents that are instantaneous, independent of voltage, and selective for K^+. Additionally, current flow through ORK1 is predominantly determined by the prevailing electrochemical gradient for K^+. These properties, shared by all K2P channels, have prompted the suggestion that K2P channels are responsible for the leak current present in excitable cells and might consequently contribute to establish and maintain membrane resting potential [13–15].

Moreover, they are targets of numerous signal transduction events that might make them essential components involved in cell excitability [16, 17]. Based on these criteria, they could be invoked as regulators of the maximum diastolic potential and may play an important role in setting the cardiac rhythm.

Heart Rhythm Increases in *Ork1* Mutants

In order to gain insight into the in vivo physiological function of a K2P channel in cardiac activity, we first analyzed heart rhythm in *Ork1* mutant larvae. Selected from public databases, we collected four lines carrying a P-element insertion in close vicinity to the *Ork1* gene (Figure 2A). *Ork1* expression, determined by RT-PCR, was dramatically reduced in P(d01340) and PBac(e02481), revealing these lines to be partial loss-of-function mutants for *Ork1* (Figure 2B). By contrast, the level of *Ork1* expression was unaffected in P(d07318) and P(d09258). Under standard conditions, heart rhythm has been shown to be steady and reproducible among individuals and can be readily recorded [18–20]. In agreement with our RT-PCR results, a 15% and 30% increase in the cardiac rhythm was observed in the two mutant lines PBac(e02481) and P(d01340), respectively (Figure 2C), whereas it was identical to control animals in the two lines where *Ork1* expression was not affected. Thus,

*Correspondence: semeriva@ibdm.univ-mrs.fr
[2] These authors contributed equally to this work.

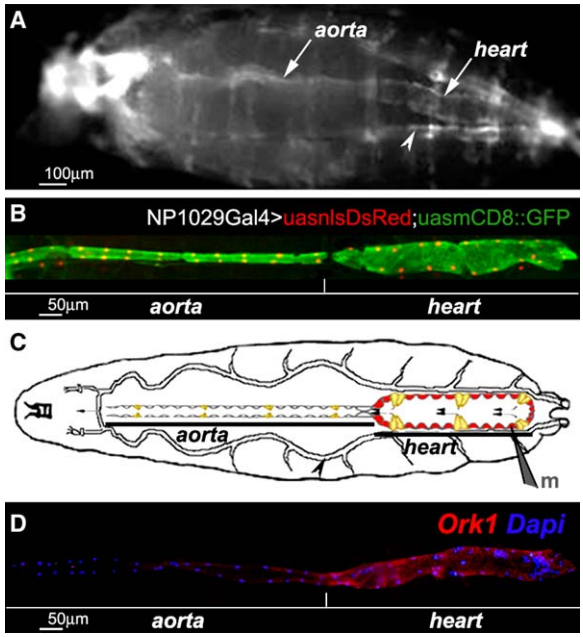

Figure 1. The *Drosophila* Cardiac Tube

(A) A cardiac tube in living white pupa labeled with NP1029-GAL4-driven membrane bound GFP showing morphological and functional differences between the aorta and the heart (see Movie S1).
(B) Expression of nuclear DsRed (red) and of membrane bound GFP (green) driven by 1029-Gal4 in late third instar larva.
(C) Schematic drawing of a third instar larval cardiac tube. The position of the microelectrode (m) for action potentials recording in the posterior heart is indicated. Arrowhead indicates tracheal tube.
(D) In situ hybridization revealed *Ork1* RNA (red) predominantly expressed in the heart (schematized in red in [C]). Nuclear labeling by DAPI (blue). Anterior is left in all panels.

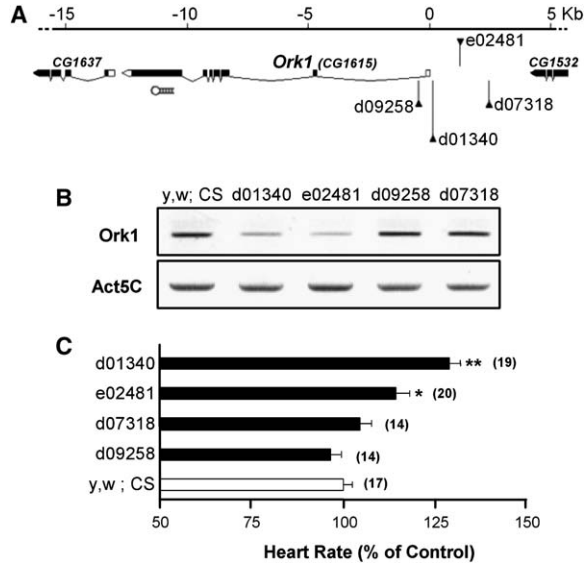

Figure 2. Heart Rate in *Ork1* Mutants

(A) Genomic organization of *Ork1*. Coding sequences are painted in black. The arrows show the positions of the P element insertions.
(B) RT-PCR for *Ork1* (top) or for the ubiquitously expressed Actin 5C gene (bottom) with RNA samples isolated from *Ork1* mutants (right) or control *y,w; CS* (left) third instar larvae.
(C) Heart rate in *Ork1* mutants was measured in white pupae. In *y,w; CS* (control), the mean heart rate was 155 ± 4 bpm (n = 17) and represents 100% of control. Two P element lines showed a significant increase of heart rhythm while the remaining two behave similarly to wild-type flies. Data are expressed as mean ± SEM. *p < 0.05; **p < 0.01.

accelerated heart rate correlates with reduction in *Ork1* expression.

Cardiac Tube-Specific *Ork1* Inactivation Accelerates Heart Rate

To address the issue of whether *Ork1* functions autonomously in the heart, *Ork1* was specifically inactivated in the cardiac tube by targeted expression of dsRNA>*Ork1* via the UAS-Gal4 system [21, 22]. Seven independent transgenic lines carrying dsRNA-*Ork1* under the control of UAS sequences were obtained and crossed with the cardiac tube-specific NP1029-Gal4 line [8]. A membrane bound GFP was coexpressed along with UAS-dsRNAs to facilitate automatic measurements of heart rate (Figure 3A, Movie S2). In the four transgenic lines that were examined thoroughly, cardiac rhythm was increased from 18% to 40% when compared to control (Figures 3B and 3D, Movie S2). The increase in heart rate was inversely correlated with the level of *Ork1* expression, determined by RT-PCR (Figure 3C). In addition, the observed acceleration in heart rhythm was correlated with the expression level of the dsRNA transgene, the effect being more pronounced at 29°C, at which temperature Gal4 is fully active, than at 21°C (Figure 3D). Importantly, *Ork1* downregulation did not lead to arrhythmia and did not significantly affect diastoles and systoles diameter (Figures 3A and 3B). The specificity of RNAi, known to be very high in *Drosophila* [23], was warranted by the congruent consequences of *Ork1* inactivation by RNAi and in *Ork1* mutants.

Arrest of Heart Beating after ORK1 Overexpression

Conversely, overexpression of wild-type *Ork1* cDNA in the whole cardiac tube during larval stages led to a complete arrest of heart beating (Figures 3A and 3B, Movie S2) and a totally dilated cardiac tube (Figure 3A). The heart beating was restored during electrical stimulation (Movie S3), indicating that ORK1-overexpressing cardiomyocytes remain excitable and have not been affected in their contractility. Arrest of heart beating was also obtained by expressing a constitutively open variant of ORK1 [12] (Figures 3A and 3B). Noteworthy is that expression of ORK1 led also to electrical silencing of the circadian pacemaker neurones [24, 25]. Together, these observations indicate that cardiac rhythm is directly correlated with ORK1 expression. A low level of ORK1 expression accelerates heart rate, whereas increasing the level of ORK1 expression completely blocks heart beating. These results strongly suggest that heart rhythm is largely influenced by ORK1-induced K^+ current.

Recording Intracellular Action Potentials Reveals that *Ork1* Determines the Rate of the Slow Diastolic Depolarization

To investigate how *Ork1* dosage manipulation affects the membrane cardiomyocytes electrical properties, we undertook the recording of intracellular action potentials by the microelectrode method, which turned out to

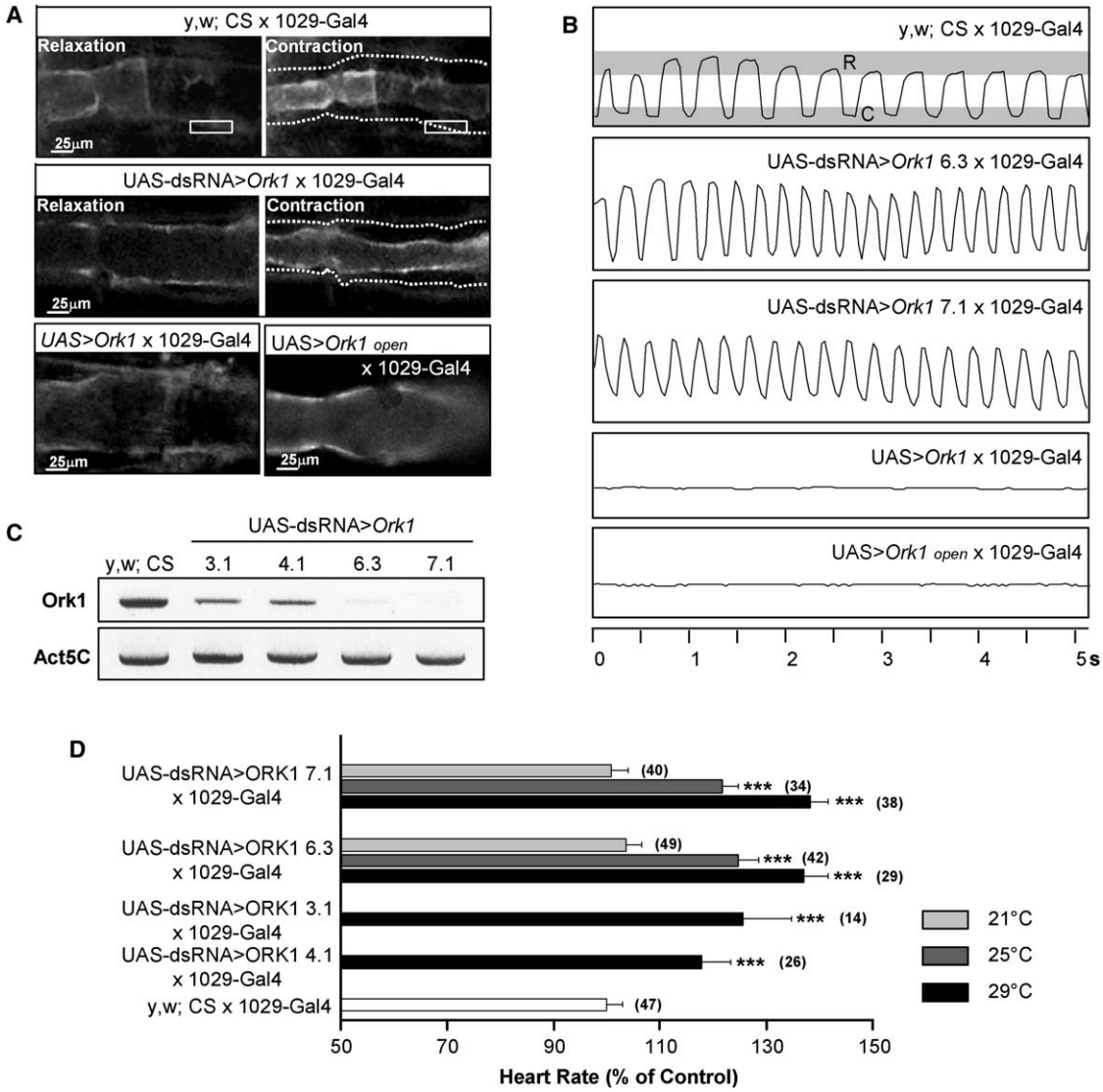

Figure 3. Heart Rate in *Ork1* Loss and Gain of Function

(A) High-magnification images of GFP-expressing larval hearts of the indicated genotypes. The amplitude of relaxation and contraction was identical in control and dsRNA>*Ork1* hearts. ORK1 and constitutively open ORK1-overexpressing hearts are completely and permanently dilated (see Movie S2).

(B) Waveforms representative of heart beatings in larvae of the indicated genotype were obtained by monitoring membrane bound GFP fluorescence in the indicated rectangles (in [A]) with the relaxation (R) and contraction (C) states indicated in (B).

(C) RT-PCR for *Ork1* (top) or for the ubiquitously expressed Actin 5C gene (bottom) with RNA samples isolated from yw; dsRNA>*Ork1; Tub>Gal4* individuals (right) or control (*y,w; ;Tub>Gal4)* (left) third instar larvae.

(D) Heart rate in *Ork1* loss of function. Heart rate was calculated in larvae as mentioned above and in the Experimental Procedures. The mean heart rate representative of 100% of control was measured in yw, CS x *1029-Gal4* third instar larvae and was 161 ± 5 bpm (n = 47). Inactivation of *Ork1* increased the heart rate. Data are expressed as mean ± SEM. ***p < 0.001.

be more reliable than the only other method hitherto reported [26]. Action potentials, corresponding to the wave of depolarization, were systematically recorded with the microelectrode implanted in the contractile myocytes of the posterior heart (at the end of the sixth segment, see Figure 1C). In those conditions, stable and reproducible action potentials were recovered (Figure 4A). In control, typical pacemaker action potentials were observed (Figure 4B) with a slow diastolic depolarization preceding the fast depolarization, which triggers contraction. The two phases of depolarization can be fitted by two exponentials, the slower one corresponding to the so-called slow diastolic depolarization (insert in Figure 4B). Several considerations ([27–29] and our own observations) suggest that the fast phase of depolarization is mainly insured by a voltage-dependent L-type calcium current. The shape of the recorded action potential was very reminiscent to that recovered in the sino-atrial node of the mammalian heart. Same types of action potentials, including the slow diastolic depolarization phase, were recorded all along the heart. Therefore, unlike in mammals, the *Drosophila* myocardium seems to be constituted by an electrophysiologically homogeneous population of cardiomyocytes

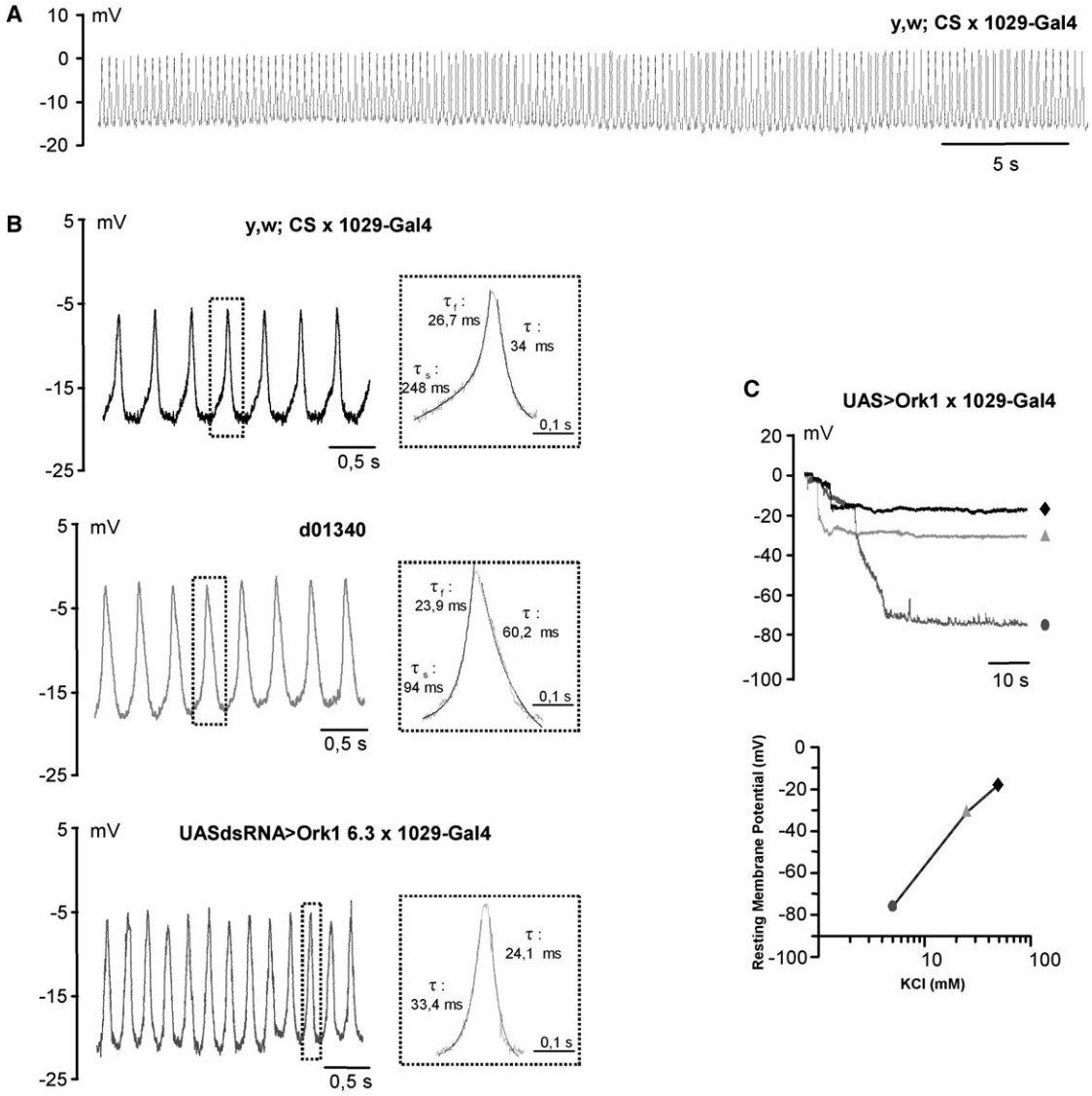

Figure 4. Role of ORK1 in Intracellular Action Potentials

(A) Intracellular recording of the electrical activity of a hemidissected heart of a control larva bathed in Schneider medium (25 mM KCl). The microelectrode was implanted in the posterior heart as indicated in Figure 1C.

(B) Top: Intracellular action potentials recorded in control larval heart in schneider medium are characterized by slow diastolic depolarization preceding fast depolarization. Insert: Fitted curves for the depolarization and repolarization phases are drawn for the indicated action potential. Middle: *Ork1* mutant shows accelerated action potentials characterized by a reduced slow diastolic depolarization phase. Bottom: *Ork1* loss of function leads to accelerated action potentials characterized by a monoexponential depolarization phase due to the absence of slow diastolic depolarization phase.

(C) Top: In the UAS>*Ork1*, no action potential was recorded. The membrane potential was stabilized to a negative value following the drop, from the zero potential reference, due to the impalement of the cell. The overexpression of *Ork1* drives the resting potential to −18, −31, and −76 mV in 5, 25, or 49 mM KCl solutions described in Experimental Procedures. Bottom: Linear regression gives a shift of 57 mV per 10-fold change in KCl concentration.

fulfilling the functions both of the mammalian working cardiomyocytes and of the cardiomyocytes with automatic activity.

Noteworthy, the value (around –18 mV) for the maximal diastolic potential was significantly higher than in mammalian sino-atrial node pacemaker, raising the question of how automatic reactivation of the action potential is induced. This high value of membrane potential, directly resulting from the physiological concentrations of K^+ in *Drosophila*, lies in fact within the window for L-type Ca^{2+} current, defined by the overlapping of activation and inactivation curves. This window current leads to permanent inward calcium influx, which would in turn be responsible for the automatic reactivation of the action potentials.

The two phases of depolarization can be fitted by two exponentials, the slower one corresponding to the so-called slow diastolic depolarization (insert in Figure 4B). In larvae where *Ork1* was inactivated, there was no statistically significant change in amplitude, maximal diastolic potential, and fast depolarization/repolarization phases (Figure 4B and Table 1). By contrast, the slow

Table 1. Averaged Characteristics of the Intracellular Action Potentials

			Amplitude (mV)		Duration (ms)		MDP (mV)		τ Depol (ms)		τ Repol (ms)	
		n	Mean	SE	Mean	SE	Mean	SE	Mean	SE	Mean	SE
1029-Gal4 ×	y,w; CS	13	−16.4	1.5	378	18.8	−17.4	2.1	227.9; 31.8	27.9; 6.3	60.3	16.2
	UAS-dsRNA 4.1	6	−13.6	2.2	269[a]	25.5	−18.4	1.3	32.9	5.3	37.6	5.8
	UAS-dsRNA 6.3	8	−16.6	1.6	249[b]	12.9	−20.3	1.8	44.8	4.8	31.6	3.2
	UAS>*Ork1*	6	0	0	0	0	−30.3[a]	3.8	0	0	0	0
d01340		9	−15.1	1.4	328[c]	7.1	−18.7	1.3	95.1[d]; 20.7	14.9; 3.8	37.0	7.9

Amplitude, duration, maximal diastolic potential (MDP), and τ are expressed as mean ± SEM and were calculated by averaging 10 individual action potentials for each experiment in schneider medium. There are no significant differences between yw;CS and 1029-Gal4 × yw;CS, which have been taken as control (results not shown). The number of experiments is indicated in the table.
[a] $p < 0.001$.
[b] $p < 0.0001$.
[c] $p < 0.04$.
[d] $p < 0.002$.

diastolic depolarization phase was significantly diminished, in d01340 mutant line, or even totally abolished in RNAi-inactivated *Ork1* (Figure 4B and Table 1). As a consequence, the increased frequency of the automatic action potential observed after *Ork1* loss of function results from a shortening of the slow diastolic depolarization phase.

Conversely, measuring the potential after ORK1 overexpression revealed a hyperpolarization of the cardiomyocytes membrane (Figure 4C), which would explain the loss of automatic cardiac activity observed. In support of this, depolarization of cardiomyocytes induced by electrical stimulation restored cardiac beating (Movie S3), indicating also that cardiomyocyte contractility was not affected. Finally, Figure 4C shows that the value of the resting membrane potential of ORK1-overexpressing cardiomyocytes varies with the external K^+ concentration according to the Nernst equation, implying that the measured membrane potential is governed by K^+ currents, most likely mediated by ORK1.

Conclusions

These results suggest that, in the *Drosophila* cardiac pacemaker, the outward K^+ current mediated by ORK1 might directly control the onset of depolarization by opposing the entry of depolarizing positive charges. However, it cannot be completely excluded that complex developmental effects that are secondary to the genetic manipulations of Ork1 contribute to the observed phenotype.

These results point out that the level of activity of a K2P channel in cardiac pacemaker can determine heart rhythm. We favor an effect on the pacemaker frequency rather than on the cardiomyocytes contractile activity. Indeed, the main modification in the course of the action potential after ORK1 activity changes lies during the early depolarization phase and not in the fast depolarization induced by L-type Ca^{2+} current. In the same line, the action potential frequency by itself shows a definite dependence on ORK1 activity, making unlikely a significant contribution of ORK1 on excitation-contraction coupling.

Strikingly, the level of ORK1 activity determines the duration of the slow diastolic depolarization without having any significant action upon the automatic activity. ORK1 appears therefore to behave as a pure regulator of the pacemaker frequency and, because of the well-known ability of K2P channels to be highly regulated by a plethora of stimuli, it might constitute a direct target for some of the known regulators of cardiac activity, such as neurotransmitters and hormones [20]. It will be particularly important to test this hypothesis and to investigate whether similar mechanisms operate in the sino-atrial node of mammalian hearts, in which the expression of different K2P channels has recently been reported [30, 31].

Experimental Procedures

Drosophila strains

UAS-mCD8-GFP, UAS-nls-DsRed, UAS>*Ork1DeltaC*, P{XP}d09258 were obtained from the Bloomington *Drosophila* Stock Centre; P{XP}d01340, P{XP}d07318, and PBac{RB}e02481 [32] from the Exelixis collection at Harvard Medical School. Gal4 driver is NP1029-Gal4 [8]. The *y,w; CS* strain, issued from a *yellow, white* strain, outcrossed with Canton S for 10 generations, was used as control. Transgenic flies were generated as previously described [33] with the *y,w; CS* strain as a recipient stock.

UAS-dsRNA>*Ork1* Constructs

A 871 bp fragment from the coding sequence (exon 7, genomic coordinates: 10622133-10621262) of the *Ork1* gene (CG1615) was PCR amplified from genomic DNA (sequence available upon request) and cloned in the pWIZ vector [22] digested by Avr II (pWIZ/*Ork1*{1}). A pWIZ/*Ork1*{1} clone was then digested by Nhe I and the 872 bp amplified product was cloned in an inverted orientation to yield to the pWIZ/*Ork1*{1,2}.

UAS>*Ork1FL* Constructs

The full-length *Ork1* cDNA [10] was excised from pRS by EcoRI digestion and inserted into EcoRI-cut pUAST transformation vector [21].

RT-PCR Experiments

Total RNA from third instar larvae was purified with Trizol (Invitrogen) according to standard procedures and reverse transcribed with the ThermoScript RT-PCR system (Invitrogen). The expression of *Ork1* and *Actin5C* (control) were analyzed with specific primers in semi-quantitative RT-PCR experiments (sequence available upon request) with Hybripol DNA polymerase (Bioline).

In Situ Hybridizations

In situ hybridizations on dissected larval individuals were performed as previously described [8].

Heart Rate Measurements

Detailed methods are available in the Supplemental Experimental Procedures online.

Electric Stimulation

In nonbeating hearts of larvae overexpressing *Ork1*, electric stimulation was applied between a platinum extracellular stimulation electrode and placed in posterior heart, and a tungsten reference electrode was located in aorta. Pacing at 2 Hz in Schneider medium was performed with a stimulator S900 and a stimulus isolation unit S910 (Dagan Corporation).

Action Potential Recordings

Larvae were carefully dissected in Schneider medium (GIBCO, Invitrogen) to preserve the integrity of the cardiac tube. Action potentials were recorded with a binocular microscope (MZ12, Leica) from the posterior part of the hemidissected heart larvae, with a standard microelectrode recording technique at 21°C. Conventional microelectrodes, with tip resistances between 20 and 40 MΩ and filled with 3 M KCl, were mounted on a 50 μm silver spiral wire to allow the microelectrode to follow cardiac motion. Action potentials were recorded as the difference in voltage between the intracellular microelectrode and the extracellular Ag-AgCl reference electrode. The signal was passed through a high-impedance amplifier (VF-180, BioLogic SA) and sampled at 2 kHz. Data acquisition and analyses were performed with Chart software (version 5.0.2, AD Instruments) and Clampfit (version 9, Axon Instruments), respectively. Heart rates recorded on dissected larvae were similar to those recorded in vivo, suggesting that Schneider medium is close to physiological conditions. KCl solutions used for resting membrane potentials analysis after ORK1 overexpression were: 5.4 mM $CaCl_2$, 15 mM $MgCl_2$, 4.8 mM $NaHCO_3$, 11 mM glucose, 5 mM tréhalose, 5 mM L-glutamine, 10 mM HEPES, and 5 mM, 25 mM, or 49 mM KCl and 66 mM, 46 mM, or 22 mM NaCl.

Statistical Analysis

Single- and two-exponential equations were fitted with Clampfit software (Axon Instruments). Data are reported as mean ± SEM. The significance between groups of data was assessed by Student's t test (for unpaired samples) and one-way analysis of variance (ANOVA test) when three or more groups were compared. Results were considered significant with p less than 0.05 (*$p < 0.05$, **$p < 0.01$, ***$p < 0.001$).

Supplemental Data

Three movies and Supplemental Experimental Procedures can be found with this article online at http://www.current-biology.com/cgi/content/full/16/15/1502/DC1/.

Acknowledgments

We acknowledge P. Bois, R. Kelly, M. Lazdunski, F. Lesage, and A. Moqrich for discussions and comments on the manuscript. We thank the Bloomington Stock Centre and Harvard Medical School for fly stocks, S.A. Goldstein for Ork1 cDNA, and the technical assistance of S. Long. F. Graziani, and P. Weber. This work was supported by the CNRS and by grants from ARC, AFM, CEFIPRA, and ACI BCMS. N.L. is supported by a grant from Fondation Lefoulon-Delalande and B.M. from the MESR.

Received: February 24, 2006
Revised: May 26, 2006
Accepted: May 26, 2006
Published: August 7, 2006

References

1. Cho, H.S., Takano, M., and Noma, A. (2003). The electrophysiological properties of spontaneously beating pacemaker cells isolated from mouse sinoatrial node. J. Physiol. *550*, 169–180.
2. DiFrancesco, D. (1995). The onset and autonomic regulation of cardiac pacemaker activity: relevance of the f current. Cardiovasc. Res. *29*, 449–456.
3. Stieber, J., Hofmann, F., Ludwig, A., Herrmann, S., Feil, S., Loster, J., Feil, R., and Biel, M. (2004). Pacemaker channels and sinus node arrhythmia. Trends Cardiovasc. Med. *14*, 23–28.
4. Snyders, D.J. (1999). Structure and function of cardiac potassium channels. Cardiovasc. Res. *42*, 377–390.
5. Lo, P.C., and Frasch, M. (2003). Establishing A-P polarity in the embryonic heart tube: a conserved function of Hox genes in *Drosophila* and vertebrates? Trends Cardiovasc. Med. *13*, 182–187.
6. Perrin, L., Monier, B., Ponzielli, R., Astier, M., and Semeriva, M. (2004). *Drosophila* cardiac tube organogenesis requires multiple phases of Hox activity. Dev. Biol. *272*, 419–431.
7. Ponzielli, R., Astier, M., Chartier, A., Gallet, A., Therond, P., and Semeriva, M. (2002). Heart tube patterning in *Drosophila* requires integration of axial and segmental information provided by the *Bithorax Complex* genes and *hedgehog* signaling. Development *129*, 4509–4521.
8. Monier, B., Astier, M., Semeriva, M., and Perrin, L. (2005). Steroid-dependent modification of Hox function drives myocyte reprogramming in the *Drosophila* heart. Development *132*, 5283–5293.
9. Stieber, J., Herrmann, S., Feil, S., Loster, J., Feil, R., Biel, M., Hofmann, F., and Ludwig, A. (2003). The hyperpolarization-activated channel HCN4 is required for the generation of pacemaker action potentials in the embryonic heart. Proc. Natl. Acad. Sci. USA *100*, 15235–15240.
10. Goldstein, S.A., Price, L.A., Rosenthal, D.N., and Pausch, M.H. (1996). ORK1, a potassium-selective leak channel with two pore domains cloned from *Drosophila melanogaster* by expression in *Saccharomyces cerevisiae*. Proc. Natl. Acad. Sci. USA *93*, 13256–13261.
11. Ilan, N., and Goldstein, S.A. (2001). Kcnko: single, cloned potassium leak channels are multi-ion pores. Biophys. J. *80*, 241–253.
12. Zilberberg, N., Ilan, N., Gonzalez-Colaso, R., and Goldstein, S.A. (2000). Opening and closing of KCNKO potassium leak channels is tightly regulated. J. Gen. Physiol. *116*, 721–734.
13. Lesage, F., Maingret, F., and Lazdunski, M. (2000). Cloning and expression of human TRAAK, a polyunsaturated fatty acids-activated and mechano-sensitive K(+) channel. FEBS Lett. *471*, 137–140.
14. Goldstein, S.A., Bockenhauer, D., O'Kelly, I., and Zilberberg, N. (2001). Potassium leak channels and the KCNK family of two-P-domain subunits. Nat. Rev. Neurosci. *2*, 175–184.
15. O'Connell, A.D., Morton, M.J., and Hunter, M. (2002). Two-pore domain K+ channels-molecular sensors. Biochim. Biophys. Acta *1566*, 152–161.
16. Besana, A., Barbuti, A., Tateyama, M.A., Symes, A.J., Robinson, R.B., and Feinmark, S.J. (2004). Activation of protein kinase C epsilon inhibits the two-pore domain K+ channel, TASK-1, inducing repolarization abnormalities in cardiac ventricular myocytes. J. Biol. Chem. *279*, 33154–33160.
17. Patel, A.J., and Lazdunski, M. (2004). The 2P-domain K+ channels: role in apoptosis and tumorigenesis. Pflugers Arch. *448*, 261–273.
18. Wessells, R.J., Fitzgerald, E., Cypser, J.R., Tatar, M., and Bodmer, R. (2004). Insulin regulation of heart function in aging fruit flies. Nat. Genet. *36*, 1275–1281.
19. Paternostro, G., Vignola, C., Bartsch, D.U., Omens, J.H., McCulloch, A.D., and Reed, J.C. (2001). Age-associated cardiac dysfunction in *Drosophila melanogaster*. Circ. Res. *88*, 1053–1058.
20. Johnson, E., Sherry, T., Ringo, J., and Dowse, H. (2002). Modulation of the cardiac pacemaker of *Drosophila*: cellular mechanisms. J. Comp. Physiol. [B] *172*, 227–236.
21. Brand, A.H., and Perrimon, N. (1993). Targeted gene expression as a means of altering cell fates and generating dominant phenotypes. Development *118*, 401–415.
22. Lee, Y.S., and Carthew, R.W. (2003). Making a better RNAi vector for *Drosophila*: use of intron spacers. Methods *30*, 322–329.
23. Boutros, M., Kiger, A.A., Armknecht, S., Kerr, K., Hild, M., Koch, B., Haas, S.A., Consortium, H.F., Paro, R., and Perrimon, N. (2004). Genome-wide RNAi analysis of growth and viability in *Drosophila* cells. Science *303*, 832–835.
24. Nitabach, M.N., Blau, J., and Holmes, T.C. (2002). Electrical silencing of *Drosophila* pacemaker neurons stops the free-running circadian clock. Cell *109*, 485–495.
25. Nitabach, M.N., Sheeba, V., Vera, D.A., Blau, J., and Holmes, T.C. (2005). Membrane electrical excitability is necessary for the free-running larval *Drosophila* circadian clock. J. Neurobiol. *62*, 1–13.

26. Papaefthmiou, C., and Theophilidis, G. (2001). An in vitro method for recording the electrical activity of the isolated heart of the adult *Drosophila melanogaster*. In Vitro Cell. Dev. Biol. Anim. *37*, 445–449.
27. Gielow, M.L., Gu, G.G., and Singh, S. (1995). Resolution and pharmacological analysis of the voltage-dependent calcium channels of *Drosophila* larval muscles. J. Neurosci. *15*, 6085–6093.
28. Eberl, D.F., Ren, D., Feng, G., Lorenz, L.J., Van Vactor, D., and Hall, L.M. (1998). Genetic and developmental characterization of *Dmca1D*, a calcium channel alpha1 subunit gene in *Drosophila melanogaster*. Genetics *148*, 1159–1169.
29. Gu, G.G., and Singh, S. (1995). Pharmacological analysis of heartbeat in *Drosophila*. J. Neurobiol. *28*, 269–280.
30. Marionneau, C., Couette, B., Liu, J., Li, H., Mangoni, M.E., Nargeot, J., Lei, M., Escande, D., and Demolombe, S. (2005). Specific pattern of ionic channel gene expression associated with pacemaker activity in the mouse heart. J. Physiol. *562*, 223–234.
31. Graham, V., Zhang, H., Willis, S., and Creazzo, T.L. (2006). Expression of a two-pore domain K+ channel (TASK-1) in developing avian and mouse ventricular conduction systems. Dev. Dyn. *235*, 143–151.
32. Thibault, S.T., Singer, M.A., Miyazaki, W.Y., Milash, B., Dompe, N.A., Singh, C.M., Buchholz, R., Demsky, M., Fawcett, R., Francis-Lang, H.L., et al. (2004). A complementary transposon tool kit for *Drosophila melanogaster* using P and piggyBac. Nat. Genet. *36*, 283–287.
33. Rubin, G.M., and Spradling, A.C. (1982). Genetic transformation of *Drosophila* with transposable element vectors. Science *218*, 348–353.